# A Predictive Current Control for a Single-Phase Matrix Converter

M. Rivera, S. Rojas
Universidad de Talca
Curico, CHILE
Email: marcoesteban@gmail.com
http://www.utalca.cl

P. Wheeler
The University of Nottingham
Nottingham, U.K.
Email: pat.wheeler@nottingham.ac.uk
http://www.nottingham.ac.uk

J. Rodriguez
Universidad Nacional Andrés Bello
Santiago, CHILE
Email: jose.rodriguez@unab.cl
http://www.unab.cl

***Abstract*—This paper presents a finite control set model predictive current control strategy with a prediction horizon of one sampling time to control the single-phase matrix converter. The proposed current control strategy is based on a prediction calculation to select the switching states of the converter. By using a predictive cost function, the optimal switching state to be applied to the next sampling time is selected. This is done in order to obtain a good tracking of the load currents to their respective references. The feasibility of the proposed strategy is verified by simulation and experimental results, which show good dynamic and stationary performance.**

NOMENCLATURE

| Variable | Description | |
|---|---|---|
| $\mathbf{v_i}$ | Input voltage | $[v_A\ v_B\ v_C]^T$ |
| $\mathbf{i_i}$ | Input current | $[i_A\ i_B\ i_C]^T$ |
| $\mathbf{v}$ | Load voltage | $v^+ - v^-$ |
| $i_o$ | Load current | |
| $C_f$ | Input filter capacitor | |

## I. INTRODUCTION

The matrix converter (MC) consists of an array of bidirectional switches, which are used to directly connect the power supply to the load without using any dc-link or large energy storage elements [1]. The most important characteristics of matrix converters are [2], [3]: 1) a simple and compact power circuit; 2) generation of load voltage with arbitrary amplitude and frequency; 3) sinusoidal input and output currents; 4) operation with unity power factor; 5) regeneration capability. These highly attractive characteristics are the reason for the tremendous interest in this topology.

The intensive research on matrix converters began with the work of Venturini and Alesina in 1980 [2]. They provided the rigorous mathematical background and introduced the name "matrix converter", elegantly describing how the low-frequency behavior of the voltages and currents are generated at the load and input. One of the biggest difficulties in the operation of this converter was the commutation of the bidirectional switches [4]. This problem has been solved by introducing intelligent and soft commutation techniques, giving new momentum to research in the area. After almost three decades of intensive research, the development of this converter is reaching industrial application [5]. In effect, at least one big manufacturer of power converters (Yaskawa) is now offering a complete line of standard units for up to several megawatts and medium voltage using cascade connection. These units have rated power (and voltages) of 9-114 kVA (200 V and 400 V) for low voltage MC, and 200-6.000 kVA (3.3 kV, 6.6 kV) for medium voltage [1]. Years of continuous effort have been dedicated to the development of different modulation and control strategies that can be applied to matrix converters [4], [6]–[12].

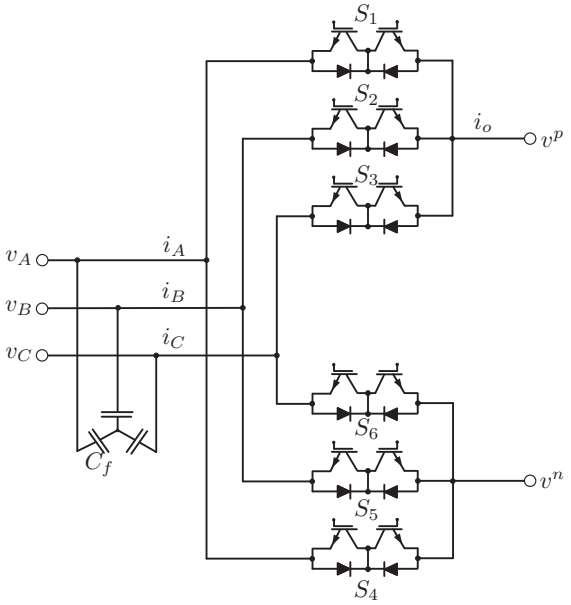


Fig. 1. Topology of the single-phase matrix converter.

Regarding the main applications of matrix converters there are two main approaches: (1) speed variation on fans and pumps that require strict control of harmonic distortion and on the other hand (2) applications with high mechanical inertia as centrifuges, cranes and mechanical stairs, in order to employ the regenerative capacity [1].

One of the latest and most successful strategies to control and modulate matrix converters is predictive control [13]. The aim of this technique is to select the best commutation state (from all the feasible ones) that minimizes a certain objective function, proposed according to the control goals. Predictive control uses the dynamic model of the system to

predict its future behavior, and, based on this prediction, the proper switching state is selected [14]. Thanks to the accurate models available for the electrical systems, the finite number of feasible commutation states of the power converters, and the fast sampling frequencies achieved with the actual digital signal processors, predictive control has emerged as one of the most effective techniques for matrix converters [15].

This paper presents a predictive current control strategy for a single-phase matrix converter. This converter is the basic cell of the converter presented in [1]. The proposed control scheme predicts the future load current behavior for each valid switching state of the converter, in terms of the measured load current and predicted load voltage. The predictions are evaluated with a cost function that minimizes the error between the predicted currents and their references at the end of each sampling time. To validate the proposed method, simulations are carried out followed by experimental results implemented in a laboratory prototype.

## II. Topology and Mathematical Model of the Single-Phase Matrix Converter

The mathematical model of the single-phase matrix converter is obtained from Fig. 1. The output voltage $v = [v^p - v^n]$ is obtained as a function of the converter's switches and the input voltages $\mathbf{v_i}$, as follows:

$$v^p = \begin{bmatrix} S_1 & S_2 & S_3 \end{bmatrix} \mathbf{v_i}, \tag{1}$$

$$v^n = \begin{bmatrix} S_4 & S_5 & S_6 \end{bmatrix} \mathbf{v_i}. \tag{2}$$

The input currents $\mathbf{i_i}$ are synthesized as a function of the converter's switches and the load current $i_o$:

$$\mathbf{i_i} = \begin{bmatrix} S_1 - S_4 \\ S_2 - S_5 \\ S_3 - S_6 \end{bmatrix} i_o. \tag{3}$$

These equations correspond to the nine valid switching states of the converter, as reported in [16], and following the restrictions of no short circuits in the input and no open lines in the output. A summary of the valid switching states of the converter and the output voltage and input currents for each switching state is presented in Table I. Finally, assuming an inductive-resistive load, the following equation describes the behavior of the load:

$$\frac{di_o}{dt} = \frac{1}{L} v - \frac{R}{L} i_o. \tag{4}$$

## III. Predictive Current Control for the Single-Phase Matrix Converter

The control scheme for the single-phase matrix converter is represented in Fig. 2. The approach pursues the selection of the switching state of the converter that leads the output current closest to its respective reference at the end of the sampling period.

First, the control objective is determined and the variables necessary to obtain the prediction model are measured and calculated. The system model and measurements are used to predict the behavior of the variable that will be controlled in the subsequent sampling time for each of the valid switching states. The predicted value is then used to evaluate a cost function which deals with the control objective.

After that, the valid switching state that produces the lowest value of the cost function is selected for the next sampling period. In order to compute the differential equation shown in eq. (4), the general forward-difference Euler formula is used as the derivative approximation to estimate the value of each function one sample time in the future.

### A. Prediction model

The output current prediction can be obtained using a forward Euler approximation in eq. (4):

$$i_o(k+1) = d_1 v(k) + d_2 i_o(k), \tag{5}$$

where, $d_1 = T_s/L$ and $d_2 = 1 - RT_s/L$ are constants dependent on load parameters and the sampling time $T_s$ [17].

### B. Cost function

The cost function is defined in equation (6), where the error between the reference and the predicted value of the output current is considered.

$$g(k+1) = (i_o^*(k+1) - i_o(k+1))^2. \tag{6}$$

The goal of cost function optimization is to achieve $g$ value close to zero. The switching state that minimizes the cost function is chosen and then applied at the next sampling instant.

Additional constraints such as current limitation and spectrum shaping can also be included in the cost function. During each sampling instant, the minimum value of $g$ is selected from the 9 function values. At $k^{th}$ instant, the algorithm selects a switching state which would minimize the cost function at the $k+1$ instant, and then applies this optimal switching state during the whole $k+1$ period.

It is worth noting that the cost function only considers the output current. However, thanks to the absence of an energy accumulator in the matrix converter, the output current control indirectly provides an input current control. In effect, as (3) shows, the input current depends only on the commutation states and the output current. Therefore, as the output current is controlled, there is no need for internal loops to limit the input current, because the proposed control ensures that the output current will not reach any prohibitive value.

## IV. Simulation and Experimental Results

The predictive current control strategy was simulated using Gecko-Circuits with the parameters indicated in Table II and the same parameters have been used for the experimental verification. All the figures are divided in two sections: a) load current (red), b) load voltaje (blue) and source voltage (purple).

In Fig. 3 simulation are presented in steady state where an output current amplitude of 6 Apk @ $f_o$=50 Hz has been imposed. The same conditions are evaluated experimentally as depicted in Fig. 4. Both simulation and experimental results

TABLE I
FEASIBLE SWITCHING STATES OF THE SINGLE-PHASE MATRIX CONVERTER

| Switching State # | $S_1$ | $S_2$ | $S_3$ | $S_4$ | $S_5$ | $S_6$ | $v^p$ | $v^n$ | $i_A$ | $i_B$ | $i_C$ |
|---|---|---|---|---|---|---|---|---|---|---|---|
| 1 | 0 | 0 | 1 | 0 | 0 | 1 | $v_C$ | $v_C$ | 0 | 0 | 0 |
| 2 | 0 | 1 | 0 | 0 | 1 | 0 | $v_B$ | $v_B$ | 0 | 0 | 0 |
| 3 | 1 | 0 | 0 | 1 | 0 | 0 | $v_A$ | $v_A$ | 0 | 0 | 0 |
| 4 | 0 | 0 | 1 | 0 | 1 | 0 | $v_C$ | $v_B$ | 0 | $-i_o$ | $i_o$ |
| 5 | 0 | 0 | 1 | 1 | 0 | 0 | $v_C$ | $v_A$ | $-i_o$ | 0 | $i_o$ |
| 6 | 0 | 1 | 0 | 0 | 0 | 1 | $v_B$ | $v_C$ | 0 | $i_o$ | $-i_o$ |
| 7 | 0 | 1 | 0 | 1 | 0 | 0 | $v_B$ | $v_A$ | $-i_o$ | $i_o$ | 0 |
| 8 | 1 | 0 | 0 | 0 | 0 | 1 | $v_A$ | $v_C$ | $i_o$ | 0 | $-i_o$ |
| 9 | 1 | 0 | 0 | 0 | 1 | 0 | $v_A$ | $v_B$ | $i_o$ | $-i_o$ | 0 |

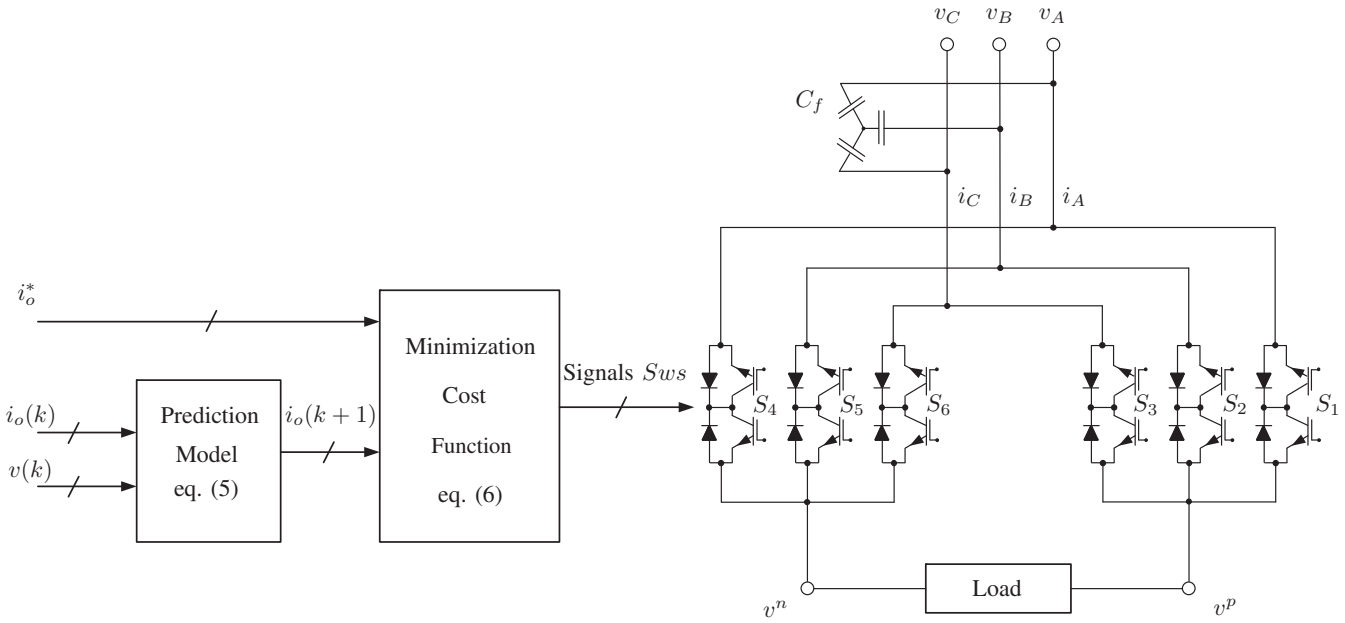


Fig. 2. Proposed control scheme for the single-phase matrix converter.

TABLE II
SIMULATION PARAMETERS

| **Variables** | **Description** | **Value** |
|---|---|---|
| $T_s$ | Sampling time | 10, 20, 40 kHz |
| $V_s$ | Source voltage | 56, 112 V |
| $f_s$ | Source frequency | 50 Hz |
| $R$ | Load resistor | 10 Ω |
| $L$ | Load inductor | 10 mH |

are obtained for a sampling frequency of $f_s$ = 20 kHz. In Fig. 5 and Fig. 6 are presented simulation and experimental results for a sampling frequency of $f_s$ = 40 kHz, respectively. In all these cases is observed a very good tracking of the load current to its reference under the different conditions.

One important issue that it is observed in the experimental results is the lower switching frequency in respect to the simulations which is evident in the figures. Transient analysis in both simulation and experimental have also been done. In Fig. 7 and Fig. 8 are shown simulation results for a step change in amplitude and frequency, respectively. The amplitude change is from 3 Apk to 6 Apk @ $f_o$ = 50 Hz and the frequency change is from $f_o$ = 50 Hz to $f_o$ = 25 Hz at a sampling frequency of $f_s$ = 10 kHz. The same analysis is done in experimental implementation as shown in Fig. 9 and Fig. 10, respectively. Again, in all these cases a very good tracking of the load current to its reference is obtained with a very fast dynamic response.

In order to assess the performance of the predictive current control scheme, two parameters are defined: the mean current tracking error and the output current THD. The percentage mean absolute current reference tracking error $\%e_{io}$ is defined as the absolute difference between the reference and load currents (for $m$ number of samples) with respect to the *rms* value of load current [18], [19]:

$$\%e_{i_o} = \frac{\frac{1}{m}\sum_{k=0}^{m}|i_o^*(k) - i_o(k)|}{rms(i_o(k))}. \tag{7}$$

In the case of the output current THD, it is defined as follows:

$$\%\,\text{THD} = \frac{\sqrt{s_2^2 + s_3^2 + .. + s_n^2}}{s_1}, \tag{8}$$

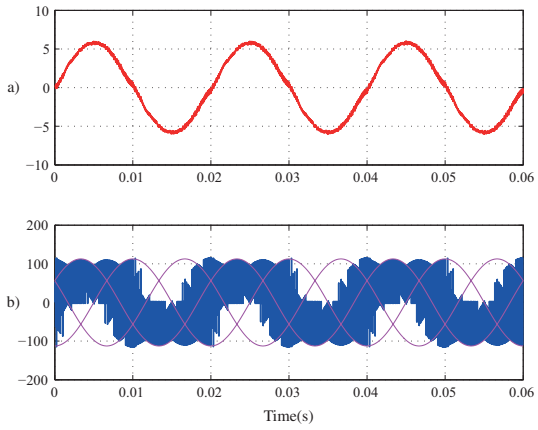


Fig. 3. Simulation results in steady state: $i_o$ = 6Apk; $f_o$ = 50 Hz; $f_s$ = 20 kHz; $v_i$ = 112 Vpk;

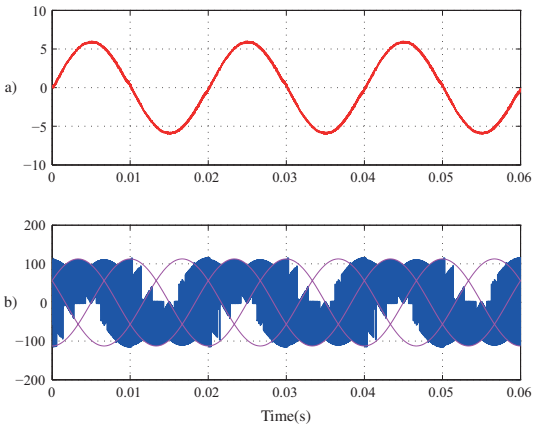


Fig. 5. Simulation results in steady state: $i_o$ = 6 Apk; $f_o$ = 50 Hz; $f_s$ = 40 kHz; $v_i$ = 112 Vpk;

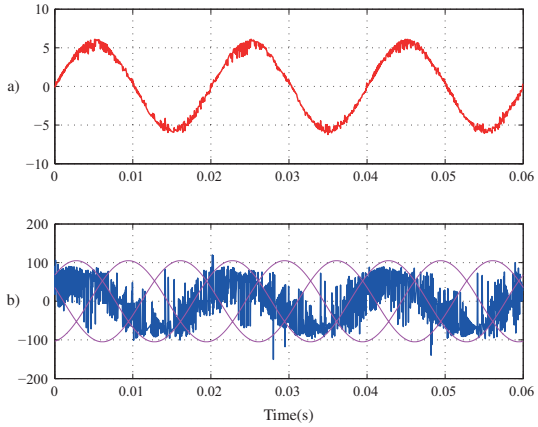


Fig. 4. Experimental results in steady state: $i_o$ = 6 Apk; $f_o$ = 50 Hz; $f_s$ = 20 kHz; $v_i$ = 112 Vpk;

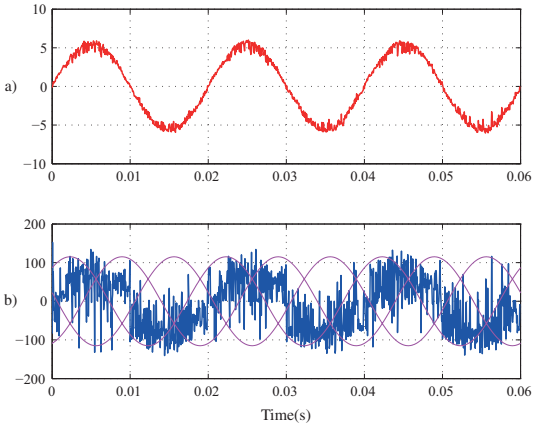


Fig. 6. Experimental results in steady state: $i_o$ = 6 Apk; $f_o$ = 50 Hz; $f_s$ = 40 kHz; $v_i$ = 112 Vpk;

where $s_n$ and $s_1$ are $n^{th}$ order harmonic and fundamental components of the signal, respectively.

Table III shows the mean average error of the load current for different sampling frequency and references evaluated in simulation and experiments. As expected, in the experiments a higher error is obtained due to some unknown parameters which are not considered in the model. The smaller error is observed when a sampling frequency of $f_s = 20kHz$ is considered. Table IV shows the THD values for simulation and experiments for the load current. Similarly, here is also observed that the lower THD value is observed for a sampling frequency of $f_s$ = 20 kHz.

From Fig. 11 to Fig. 14 are presented simulation and experimental results under frequency and amplitude variations. There is observed a very good dynamic responde without any significant overshoot or delay. With these results, the feasibility of the proposed strategy is demonstrated, with no modulators and linear controllers needed, obtaining very good dynamic response with only the prediction of the output current for each valid switching state and the optimization of the cost function at every sampling time $T_s$.

TABLE III
MEAN AVERAGE ERROR OF$i_{ref}$ VERSUS $i_o$ A UNA $f_o$ = 50 HZ

| **Sampling** ($f_s$) | **Amplitude** ($i_o$) | **Error** ($e_{sim}$) | **Error** ($e_{exp}$) |
|---|---|---|---|
| 10 kHz | 2 Apk | 6,994% | 8,294% |
| 10 kHz | 6 Apk | 4,732% | 6,640% |
| 20 kHz | 2 Apk | 4,192% | 5,541% |
| 20 kHz | 6 Apk | 2,869% | 4,796% |
| 40 kHz | 2 Apk | 2,097% | 5,181% |
| 40 kHz | 6 Apk | 1,425% | 5,112% |

## V. CONCLUSION

A current control for a single-phase matrix converter has been presented in this paper. The control scheme uses the predicted values of the output currents to evaluate the best-suited converter state considering the output current error in a cost function. Predictive control can prevent the need to use complex modulation techniques and internal cascade loops. The gate drive signals for the power switches are generated directly by the controller. Our results demonstrated that the

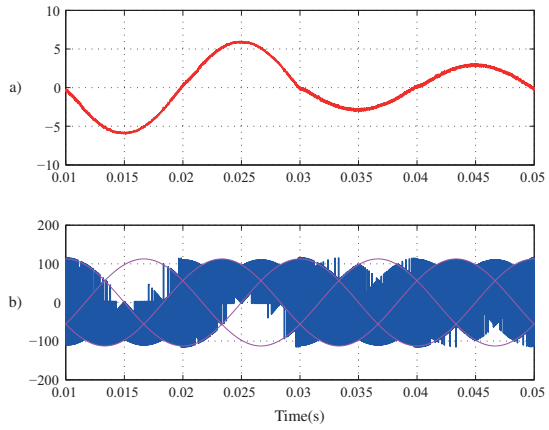


Fig. 7. Simulation results in transient state: $i_o$=3-6 Apk; $f_o$ = 50 Hz; $f_s$ = 10 kHz; $v_i$ = 112 Vpk;

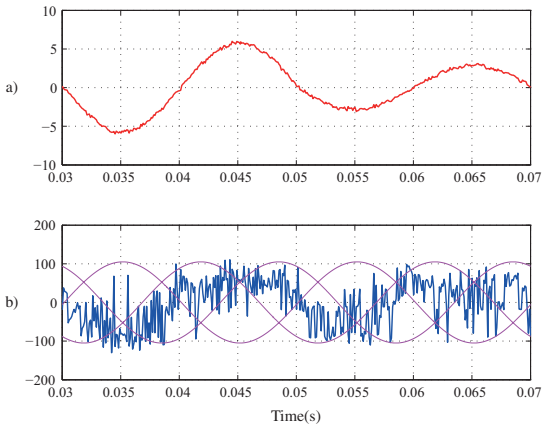


Fig. 9. Experimental results in transient state: $i_o$ = 3-6 Apk; $f_o$ = 50 Hz; $f_s$ = 10 kHz; $v_i$ = 112 Vpk.

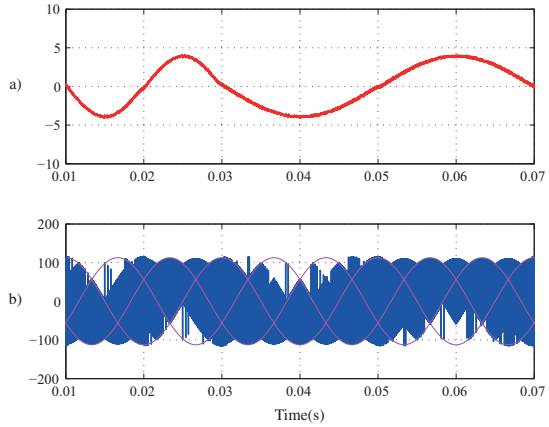


Fig. 8. Simulation results in transient state: $i_o$ = 4 Apk; $f_o$ = 50-25 Hz; $f_s$ = 20 kHz; $v_i$ = 112 Vpk;

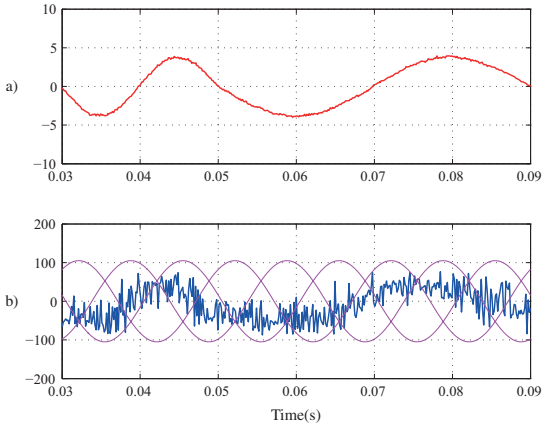


Fig. 10. Experimental results in transient state: $i_o$ = 4 Apk; $f_o$ = 50-25 Hz; $f_s$ = 20 kHz; $v_i$ = 112 Vpk;

TABLE IV
TOTAL HARMONIC DISTORTION OF THE LOAD CURRENT @ $f_o$ = 50 HZ

| **Sampling** ($f_s$) | **Amplitude** ($i_{ref}$) | **THD Sim.** ($i_o$) | **THD Exp.** ($i_o$) |
|---|---|---|---|
| 10 kHz | 2 Apk | 12,534% | 11,572% |
| 10 kHz | 6 Apk | 7,235% | 10,121% |
| 20 kHz | 2 Apk | 6,608% | 7,830% |
| 20 kHz | 6 Apk | 4,387% | 6,923% |
| 40 kHz | 2 Apk | 3,465% | 10,307% |
| 40 kHz | 6 Apk | 2,376% | 8,837% |

presented strategy provides good tracking of the output current to its reference.

## ACKNOWLEDGMENTS

This publication was made possible by the Newton Picarte Project EPSRC: EP/N004043/1: New Configurations of Power Converters for Grid Interconnection Systems / CONICYT DPI20140007 and British Council through the Institutional Skills Development Newton Picarte Project ISCL 2015006.

## REFERENCES

[1] E. Yamamoto, T. Kume, H. Hara, T. Uchino, J. Kang, and H. Krug, "Development of matrix converter ans its applications in industry," *35th Annual Conference of the IEEE Industrial Electronics Society IECON 2009, Porto, Portugal*, 2009.

[2] M. Venturini, "A new sine wave in sine wave out, conversion technique which eliminates reactive elements," *Powercon 7, 1980*, pp. E3/1–E3/15, Mar. 2001.

[3] J. Rodriguez, E. Silva, F. Blaabjerg, P. Wheeler, J. Clare, and J. Pontt, "Matrix converter controlled with the direct transfer function approach: analysis, modelling and simulation," *Taylor and Francis-International Journal of Electronics*, vol. 92, no. 2, pp. 63 –85, Feb. 2005.

[4] L. Zhang, C. Watthanasarn, and W. Shepherd, "Control of ac-ac matrix converters for unbalanced and/or distorted supply voltage," *Power Electronics Specialists Conference, 2001. PESC. 2001 IEEE 32nd Annual*, vol. 2, pp. 1108 –1113 vol.2, 2001.

[5] E. Yamamoto, H. Hara, T. Uchino, M. Kawaji, T. Kume, J. K. Kang, and H.-P. Krug, "Development of mcs and its applications in industry [industry forum]," *Industrial Electronics Magazine, IEEE*, vol. 5, no. 1, pp. 4 –12, march 2011.

[6] G. Roy and G.-E. April, "Cycloconverter operation under a new scalar control algorithm," *Power Electronics Specialists Conference, 1989. PESC '89 Record., 20th Annual IEEE*, pp. 368 –375 vol.1, Jun. 1989.

[7] J. Rodriguez, "High performance dc motor drive using a pwm rectifier

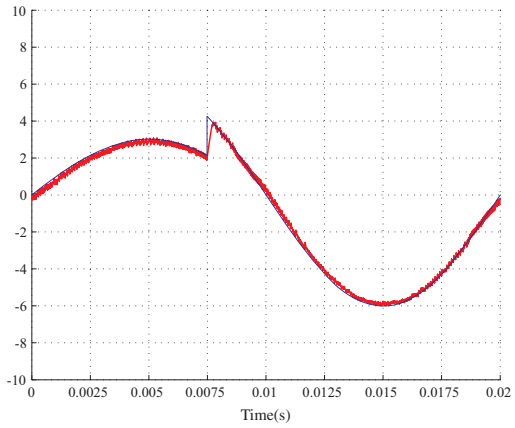


Fig. 11. Simulation results in transient state: $i_o$ = 3-6 Apk; $f_o$ = 50 Hz; $f_s$ = 40 kHz; $v_i$ = 112 Vpk;

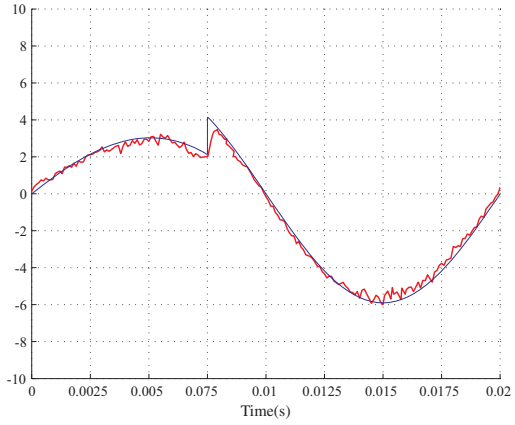


Fig. 12. Experimental results in transient state: $i_o$ = 3-6 Apk; $f_o$ = 50 Hz; $f_s$ = 40 kHz; $v_i$ = 112 Vpk;

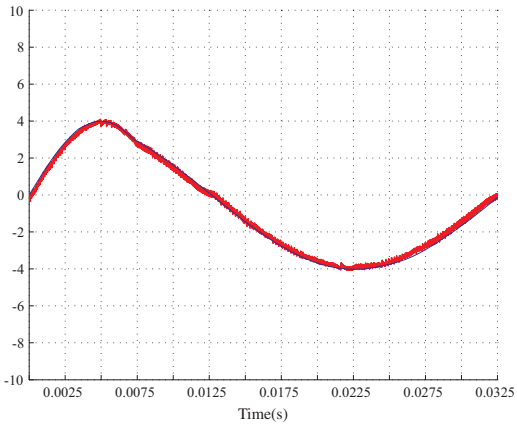


Fig. 13. Simulation results in transient state: $i_o$ = 4 Apk; $f_o$ = 50-25 Hz; $f_s$ = 40 kHz; $v_i$ = 112 Vpk;

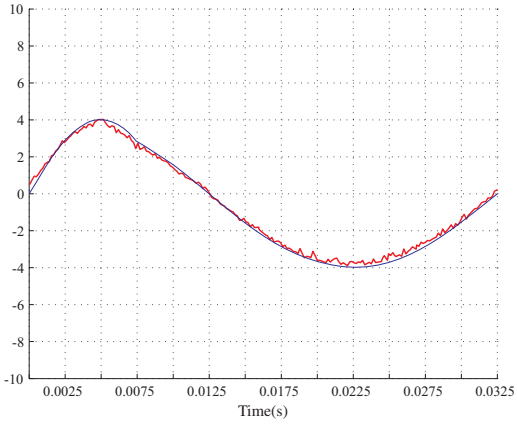


Fig. 14. Experimental results in transient state: $i_o$ = 4 Apk; $f_o$ = 50-25 Hz; $f_s$ = 40 kHz; $v_i$ = 112 Vpk;


with power transistors," *Electric Power Applications, IEE Proceedings B*, vol. 134, no. 1, p. 9, Jan. 1987.

[8] L. Huber and D. Borojevic, "Space vector modulated three-phase to three-phase matrix converter with input power factor correction," *Industry Applications, IEEE Transactions on*, vol. 31, no. 6, pp. 1234 –1246, Nov. 1995.

[9] F. Blaabjerg, D. Casadei, C. Klumpner, and M. Matteini, "Comparison of two current modulation strategies for matrix converters under unbalanced input voltage conditions," *Industrial Electronics, IEEE Transactions on*, vol. 49, no. 2, pp. 289 –296, Apr. 2002.

[10] I. Takahashi and T. Noguchi, "A new quick response and high efficency control strategy for an induction motor," *Industrial Electronics, IEEE Transactions on*, vol. 22, no. 5, pp. 820 –827, Sep. 1986.

[11] S. Muller, U. Ammann, and S. Rees, "New time-discrete modulation scheme for matrix converters," *Industrial Electronics, IEEE Transactions on*, vol. 52, no. 6, pp. 1607 – 1615, Dec. 2005.

[12] M. Rivera, R. Vargas, J. Espinoza, and J. Rodriguez, "Behavior of the predictive dtc based matrix converter under unbalanced ac-supply," *Power Electronics Specialists Conference, 2008. PESC 2008. IEEE*, pp. 202 –207, Sep. 2007.

[13] M. Rivera, C. Rojas, J. Rodriguez, P. Wheeler, B. Wu, and J. Espinoza, "Predictive current control with input filter resonance mitigation for a direct matrix converter," *IEEE Trans. Power Electron.*, vol. 26, no. 10, pp. 2794–2803, Oct. 2011.

[14] S. Kouro, P. Cortes, R. Vargas, U. Ammann, and J. Rodriguez, "Model predictive control-A simple and powerful method to control power converters," *IEEE Trans. Ind. Electron.*, vol. 56, no. 6, pp. 1826–1838, Jun. 2009.

[15] J. Rodriguez, M. P. Kazmierkowski, J. R. Espinoza, P. Zanchetta, H. Abu-Rub, H. A. Young, and C. A. Rojas, "State of the art of finite control set model predictive control in power electronics," *IEEE Trans. Ind. Informat.*, vol. 9, no. 2, pp. 1003–1016, May. 2013.

[16] C. Rojas, J. Rodriguez, A. Iqbal, H. Abu-Rub, A. Wilson, and S. Moin Ahmed, "A simple modulation scheme for a regenerative cascaded matrix converter," in *IECON 2011 - 37th Annual Conference on IEEE Industrial Electronics Society*, nov. 2011, pp. 4361 –4366.

[17] J. Rodriguez and P. Cortes, *Predictive Control of Power Converters and Electrical Drives*, 1st ed. Chichester, UK: IEEE Wiley press, Mar. 2012.

[18] V. Yaramasu, M. Rivera, B. Wu, and J. Rodriguez, "Model predictive current control of two-level four-leg inverters - part I: Concept, algorithm and simulation analysis," *IEEE Trans. Power Electron.*, vol. 28, no. 7, pp. 3459–3468, Jul. 2013.

[19] M. Rivera, V. Yaramasu, J. Rodriguez, and B. Wu, "Model predictive current control of two-level four-leg inverters - part II: Experimental implementation and validation," *IEEE Trans. Power Electron.*, vol. 28, no. 7, pp. 3469–3478, Jul. 2013.